Quantitative analysis of scour around inline and eccentric pier under fixed inflow depth

A thesis submitted towards partial fulfilment of the requirements for the degree of

Master of Engineering
in
Water Resources and Hydraulic Engineering

Submitted by

PIYUSH PRASAD GAHLAUT

Exam Roll No. – M4WRE22007
Registration No. -154647 of 2020-2021

Under the guidance of

Dr. RAJIB DAS
Assistant Professor
&
Dr. SUBHASISH DAS
Associate Professor

School of Water Resources Engineering, Jadavpur University
School of Water Resources Engineering
M.E. (Water Resources & Hydraulic Engineering)
Course affiliated to ***Faculty of Interdisciplinary Studies, Law & Management***

Jadavpur University
Kolkata-700032, West Bengal, India
2022

Declaration of Originality and Compliance of Academic Ethics

I hereby declare that this thesis contains literature survey and original research work by the undersigned candidate, as part of my **Master of Engineering** in **Water Resources and Hydraulic Engineering** in the Faculty Council of Interdisciplinary Studies, Law & Management, Jadavpur University during academic session 2020-22.

All information in this document have been obtained and presented in accordance with academic rules and ethical conduct.

I also declare that, as required by these rules and conduct, I have fully cited and referenced all material and results that are not original to this work.

Name	**:**	**Piyush Prasad Gahlaut**
Exam Roll Number	**:**	**M4WRE22007**
Thesis Title	**:**	**Quantitative analysis of scour around inline and eccentric pier under fixed inflow depth**
Signature with Date	**:**	

M.E. (Water Resources & Hydraulic Engineering)
course affiliated to
Faculty of Interdisciplinary Studies, Law & Management
Jadavpur University
Kolkata, India

Certificate of Recommendation

This is to certify that the thesis entitled "***Quantitative analysis of scour around inline and eccentric pier under fixed inflow depth***" is a Bonafide work carried out by **Mr. Piyush Prasad Gahlaut,** under our supervision and guidance for partial fulfilment of the requirement for the Post Graduate Degree of Master of Engineering in Water Resources and Hydraulic Engineering during the academic session 2020-22.

THESIS ADVISOR
Dr. Rajib Das
Assistant Professor
School of Water Resources Engineering
Jadavpur University

THESIS ADVISOR
Dr. Subhasish Das
Associate Professor
School of Water Resources Engineering
Jadavpur University

Prof. (Dr.) Pankaj Kumar Roy
DIRECTOR
School of Water Resources Engineering
Jadavpur University

Prof. (Dr.) Subenoy Chakraborty
DEAN
Faculty of Interdisciplinary Studies, Law & Management
Jadavpur University

M.E. (Water Resources & Hydraulic Engineering)
course affiliated to
Faculty of Interdisciplinary Studies, Law & Management
Jadavpur University
Kolkata, India

CERTIFICATE OF APPROVAL **

This foregoing thesis is hereby approved as a credible study of an engineering subject carried out and presented in a manner satisfactorily to warranty its acceptance as a prerequisite to the degree for which it has been submitted. It is understood that by this approval the undersigned do not endorse or approve any statement made or opinion expressed or conclusion drawn therein but approve the thesis only for purpose for which it has been submitted.

Committee of

Final Examination

for the evaluation

of the thesis

** Only in case the thesis is approved.

ACKNOWLEDGEMENT

I express my sincere gratitude to my supervisors, ***Dr. Rajib Das****, Assistant Professor and* ***Dr. Subhasish Das,*** *Associate Professor, School of Water Resources Engineering, Jadavpur University, under whose supervision and guidance this work has been carried out. It would have been impossible to carry out this thesis work with confidence without their wholehearted involvement, advice, support and constant encouragement throughout. They have not only helped me in carrying out my thesis but also have given valuable advice to proceed further in my life.*

I would also express my sincere thanks to ***Mr. Buddhadev Nandi,*** *Research Scholar; of School of Water Resources Engineering, Jadavpur University for his unconditional support and affection during my work. Also, thanks to my classmate* ***Mr. Himangshu Roy*** *for his help.*

Thanks, are also due to all staff of School of Water Resources Engineering and the Regional -cum-Facilitation Centre (RCFC), NMPB, Jadavpur University for their help and support.

Date :

Place : Jadavpur University

Mr. Piyush Prasad Gahlaut
(Exam Roll No: M4WRE22007)

ABSTRACT

Scouring is a natural phenomenon generated by the passage of water in a river or stream. It is most noticeable in alluvial materials, but severely worn rock can also be vulnerable under specific conditions. Every year, numerous bridges fail, resulting in the loss of lives and property as well as some uncomfortable circumstances for transportation systems. Because of this, bridge designers are increasingly considering the flow-soil-structure interaction. Urban setting around the world is getting densely populated and facing heavy traffic with increased number in vehicles. This opens the scope for the construction of new bridges beside already existing old ones and thus arises the need to study the interference of inline and eccentric piers. Therefore, a thorough investigation of scour depth around inline and eccentric piers in such conditions is highly desirable.

In this present study, the hydrodynamic consequences of different eccentric arrangements on scouring were investigated. Erosion and deposition patterns were studied around the front and eccentric piers at different time intervals along the flume. In these series of experiments two identical circular piers are used to conduct six experiments with fixed inflow depth and varying the eccentricity between two piers in each experiment. The longitudinal spacing between the upstream pier and the eccentric pier was also kept fixed. Six different eccentricities were used to run the experiment for 12 hours to obtain resultant scour. A fixed discharge of 27 Lps and clear water condition was also maintained throughout the experiments. The results obtained from the series of experiments was carefully analyzed to obtain the best arrangement for eccentricity which would be beneficial aspect for bridge designers.

CONTENT

NOTATION

The following symbols are used in this dissertation work:

A = (hB)Cross-sectional area of flow [L^2];

a_{ps} = Planar area of scour [L^2];

a_{ss} = Surface area of scour [L^2];

a_s = Scour area [L^2];

b = Pier diameter or width [L];

B = Width of the tilting flume [L];

d_e = Eccentric pier scour depth [L];

d_{ec} = Computed eccentric pier scour depth [L];

d_{em} = Measured eccentric pier scour depth [L]:

d_{se} = Equilibrium scour depth at eccentric pier [L]:

d_f = In-line front pier scour depth [L];

d_{fc} = Computed front pier scour depth [L];

d_{fm} = Measured front pier scour depth [L]:

d_{sf} = Scour depth at front pier [L]:

d_{se} = Scour depth at eccentric pier [L];

d_{16} = 16% finer sand diameter [L];

d_{50} = Median diameter of sand [L];

d_{84} = 84% finer sand diameter [L];

d_{90} = 90% finer sand diameter [L];

F_r = Froude number of flow [—];

F_d = Densimetric Froude number [—];

F_t = $\left(\frac{U}{u_c}\right)$ Threshold Froude number [—];

g = Gravitational acceleration [LT^{-2}];

h = Approaching flow depth [L];

h/b = Non-dimensional inflow depth [—];

i, k = Direction indices along *x* and *z* axis respectively [—];

L = Piers spacing [L];

l = Total length of scour for single pier [L];

l_s = Scour length [L];

l_{sm} = Maximum scour length [L];

L_{se} = Eccentric Pier scour length [L];

L_{sf} = Front Pier scour length [L];

n = Manning's co-efficient of roughness [—];

P = Wetted perimeter [L];

Q = Discharge [$L^3\ T^{-1}$];

r = correlation coefficient [—];

R = $\left(=\frac{A}{P}=\frac{hB}{2h+B}\right)$ Hydraulic radius[L];

R_e = $\left(\frac{UH}{\nu}\right)$ Flow Reynolds number [—];

R_{*c} = $\left(\frac{u_{*c}R}{\nu}\right)$ Critical shear flow Reynolds number [—];

R_p = $\left(\frac{Ub}{\nu}\right)$ Pier Reynolds number [—];

S = $(3b)$ Eccentricity [L];

S_0 = Bed slope [—];

s = $\left(\frac{\rho_s}{\rho_f}\right)$ Relative density of sand [—];

U = Depth-averaged approaching flow velocity [LT^{-1}];

u = Time-averaged tangential velocity[LT^{-1}];

u_c = Critical velocity [LT^{-1}];

u_* = Shear velocity [LT^{-1}];

u_{*c} = Critical shear velocity [LT^{-1}];

v = Time-averaged radial velocity[LT^{-1}];

V = $\left(\sqrt{u^2+v^2+w^2}\right)$ Time-averaged absolute velocity [LT^{-1}];

$\mathbf{V}$ = $\left(\sqrt{v^2+w^2}\right)$ Time-averaged velocity vector[LT^{-1}];

$\forall_s$ = Volume of the scour hole [L^3];

V_s = Volume of scour [L^3];

w_{se} = width of scour at eccentric pier [L];

w_{sf} = width of scour at front pier [L];

w = Time-averaged vertical velocity in the *z*-direction [LT^{-1}];

w_s = Scour width [L];

w_{sm} = Maximum scour width [L];

w_{ss} = Single pier scour width [L];

Δr = Spacing of the grid points in the radial direction [L];

Δz = Spacing of the grid points in the vertical direction [L];

ω = vorticity [T^{-1}];

ω_y = y -component of vorticity [T^{-1}];

Δ = $s-1$[—];

ρ_f = Mass density of fluid [ML^{-3}];

ρ_s = Mass density of sand [ML^{-3}];

γ_f = Specific weight of fluid[$ML^{-2}T^{-2}$];

Γ = Circulation [L^2T^{-1}];

τ_o = Average bed shear stress [$ML^{-1}T^{-2}$];

τ_{oc} = Critical bed shear stress on horizontal bed [$ML^{-1}T^{-2}$];

σ_g = Geometric standard deviation [—];

ν = Kinematic viscosity [L^2T^{-1}];

φ_r = Dynamic angle of repose [—];

Θ_c = Critical Shield's parameter [—];

T = Time scale; and

t = Time (h).

Chapter 1

1.1 Introduction

Scour is a natural phenomenon generated by rushing water's erosive impact on the bed and banks of alluvial rivers. Scour, in other terms, is the erosion of streambed silt around a barrier in a flow field. Cheremisinoff *et al.* (1987) defined scour as the lowering of the river bed due to water erosion, which has the potential to expose the foundations of structures such as bridges. Scour was characterized by Breusers *et al.* (1977) as a natural phenomenon created by the movement of water in rivers and streams. The scouring mechanism may endanger the structural integrity of hydraulic structures including bridges. When the foundation of the structures is compromised, this might lead to ultimate failure. A succession of bridge failures during floods caused by pier scour have highlighted the significance of developing better methods of protecting bridges from the ravages of scour. Bridge construction in alluvial channels causes the waterway at the bridge site to constrict. The waterway's shrinking could produce substantial scour at that location. According to Hoffmans and Verheij (1997), local scour around bridge piers and foundations caused by flood flows is the leading cause of bridge failure. Among those who have worked on pier scour are Raudkivi and Ettema (1983), Ahmed and Rajaratnam (1998), Chiew and Melville (1987), and Breusers *et al.* (1977). In their laboratory investigation on flow past cylindrical piers set on smooth, bumpy, and movable beds, Ahmed and Rajaratnam (1998) evaluated the flow around bridge piers. Jia *et al.* (2002) published the results of a numerical modelling study that simulated the time-dependent scour development around a cylindrical pier built on a loose substrate in an open channel. Chiew and Lim (2001). Link and Zanke (2004) investigated the time-dependent development of scour-hole volume at a circular pier in uniform coarse sand and produced a mathematical link between the scour volume and the maximum scour depth for water depth to pier diameter ratios ranging from one to two. However, just as scour depth is crucial in scour research, so is the time taken to reach a specific scour depth, because scour holes take time to form. As a result, it is vital to comprehend the evolution of the local scour hole over time.

Every year, numerous bridges fail, resulting in the loss of lives and property as well as some uncomfortable circumstances for transportation systems. The potential losses from bridge failures, as well as the necessity to protect against them, have encouraged a greater knowledge of the scour process, as well as improved scour prediction methods and equations. Under-prediction of pier scour depth can result in bridge failure, whereas over-prediction results in excessive resource spending in terms of building expenses. Because of this, bridge designers are increasingly considering the flow-soil-structure interaction. Achieving the safest design in light of local and regional characteristics is the most crucial factor to take into account at this stage. This is typically based on calculations of the maximum scour depth at bridge structural components and the geometrical features of the scour hole surrounding them.

The flow conditions, sediment characteristics, structure characteristics, and scouring duration are the main factors affecting the scour and deposition around the structure. As the number of structures in a river increase, the interaction between the structures will have a stronger impact on the surrounding bed profile. Local scour can be classified as "clear-water scour" or "live-bed scour." In clear water scour, bed materials are removed from the scour hole but not replenished by the approach flow, whereas in live-bed scour, the scour hole is constantly supplied with sediment by the approach flow and an equilibrium is reached when the average amount of sediment transported into the scour hole by the approach flow equals the average amount of sediment removed from the scour hole over time. Under these conditions, the local scour depth changes around a mean value on a regular basis. The interplay of flow around a bridge pier and the erodible sediment substrate surrounding is quite complex.

In this study, the scour characteristics around two circular piers- placed eccentrically to each other were investigated. All the experiments were carried out in an experimental channel at Fluvial Hydraulic Laboratory of School of Water Resources Engineering, Jadavpur University. The study was confined to uniform cohesion less material and clear-water flow conditions.

1.2 Scouring around piers

Scouring is a natural phenomenon generated by the passage of water in a river or stream. It is most noticeable in alluvial materials, but severely worn rock can also be vulnerable under specific conditions. It is caused by the erosive action of flowing water, which dissolves and erodes material from the stream bed and banks, as well as the vicinity of bridge piers and abutments. Scouring happens naturally as a result of river morphology changes and as a result of man-made structures. The following are the primary causes of scour:

(1) Depth of flow

(2) Pier width

(3) Velocity

(4) Froude number

(5) Bed materials

One of the primary reasons of bridge failure is scour. The scour destroys the bed materials around the bridge's foundation, exposing the foundation and jeopardizing the bridge's stability.

1.3 Classification of scour

Regardless of whether a structure is present, general scour happens in a river or stream as a result of natural processes. Man-made buildings or any other hazard may also induce scour in the river bed. Scour is divided into two types: (a) widespread scour and (b) localised scour. In addition, further sub-divisions of scour are depicted in Fig 1.

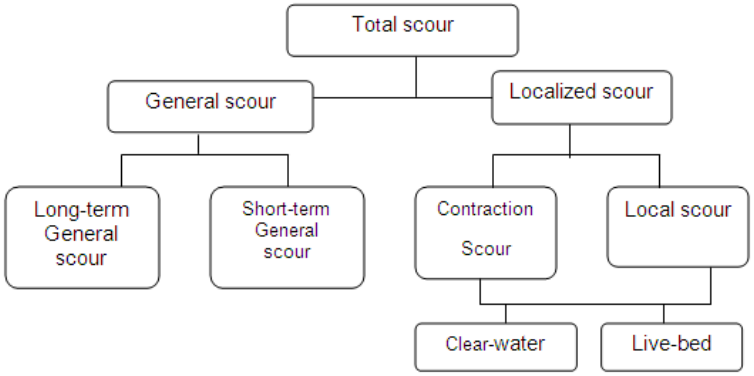

Fig 1 types of scour

1.4 Local Scour

Local scour is the erosion that takes place close to a pier, an abutment, an erosion control device, or another obstruction to the flow. These impediments speed up the flow and produce vortices that sweep the surrounding sediments away. Local scour depths are typically ten times greater than general or contraction scour depths in most cases. Local scour can cause failures by impairing the stability of riprap revetments and other structures. The following variables influence local scour:

1) Width of the obstruction.
2) Projection length of the obstruction into the flow.
3) Length of the obstruction.
4) Angle of the approach flow
5) Velocity of the approach flow
6) Size of the bed material.
7) Depth of flow.
8) Shape of the obstruction.
9) Bed configuration.

The depth of the scour is directly dependent on the width of obstruction. Thus, the wider the obstruction, the deeper is the scour. Though not addressed by most empirical relations, the ratio of obstruction width to channel width is probably a better measure of scour potential than is the obstruction width alone. Projected length of an obstruction into the stream affects the depth of scour. With an increase in the projected length of an abutment into the flow, there is an increase in scour.

Fig.2 local scour around two eccentric piers

The depth of the scour can increase with length, but only to a certain point. When the ratio of the projected length into the stream to the depth of the approaching flow is approximately 25, this limit is reached (U.S. Federal Highway Administration 1990). For straight sections, a structure's streamwise length has no discernible impact on the scour depth; however, when the structure is at an angle to the flow, the length has a significant impact. When a structure's length is doubled, the scour depth rises by as much as 33% at the same angle of attack. Some equations incorporate the length factor by using the ratio of the structure's length to the flow's depth or width as well as the flow's angle of attack on the structure. Others incorporate flow in their equations using the projected area of the structure.

The scour depth can rise by a factor of 2 or more with an increase in flow depth. Depending on the shape of the abutment, the increase for bridge abutments ranges from 1.1 to 2.15. Along with the approach flow's velocity, scour depth also rises. Although the effect is typically a function of the time exposed to erosive flows, the size of the bed material affects scour depth. In other words, only the time it takes to reach the maximum or ultimate scour may be impacted by sediment size. Large particles in the bed material, like boulders or cobbles, may armor the scour hole's plate.

Local scour is greatly influenced by the shape of the structure as well as the flow's angle of attack on an obstruction. Structures that are angled to cause flow convergence tend to increase scour, whereas structures that are angled to cause flow divergence tend to reduce scour. Streamlined structures effectively lower ultimate scour depths by weakening the horseshoe and wake vortices. The shape of the bed (bed configuration) in streams with sand beds influences the flow velocity and turbulence, which in turn influences the depth of scour. Both the local and global (contraction) scour can be accelerated by ice and debris. The extent of the growth is still largely unknown.

1.5 Vorticity

Vorticity is a concept used in fluid dynamics. In the simplest sense, vorticity is the tendency for elements of the fluid to "spin".

More formally, vorticity can be related to the amount of "circulation" or "rotation" (or the local angular rate of rotation) in a fluid. The average vorticity (ω) in a small region of fluid flow is equal to the circulation (Γ) around the boundary of the small region, divided by the area (A) of the small region.

$$\omega = \frac{\partial v}{\partial z} - \frac{\partial w}{\partial r} = \frac{\Gamma}{A} \qquad \ldots(1.1)$$

Notionally, the vorticity at a point in a fluid is the limit as the area of the small region of fluid approaches zero at the point:

$$\omega = \frac{\mathrm{d}\Gamma}{dA} \qquad \ldots(1.2)$$

Mathematically, vorticity is a vector field and is defined as the curl of the velocity field:

$$\vec{\omega} = \vec{\nabla} \times \vec{u} \qquad \ldots(1.3)$$

In fluid dynamics, vorticity is the curl of the fluid velocity. It can also be considered as the circulation per unit area at a point in a fluid flow field. It is a vector quantity, whose direction is along the axis of the fluid's rotation. For a two-dimensional flow, the vorticity vector is perpendicular to the plane.

For a fluid having locally a "rigid rotation" around an axis (i.e., moving like a rotating cylinder), vorticity is twice the angular velocity of a fluid element. An irrotational fluid has no vorticity. Somewhat counter-intuitively, an irrotational

fluid can have a non-zero angular velocity (e.g. a fluid rotating around an axis with its tangential velocity inversely proportional to the distance to the axis has a zero vorticity).

1.6 Circulation

The *Circulation* (Γ) is defined as the integral of the velocity vector around a closed path, i.e.

$$\Gamma = \oint_c V.ds = \iint_A \omega dA \qquad \text{...(1.4)}$$

The existence of closed streamlines in a flow pattern implies that there are loops for which $\Gamma \neq 0$ and thus that the flow is not irrotational everywhere. The circulation, Γ of the vortex can be estimated at different azimuthal planes from the vorticity contours by using Stokes theorem, where V is the velocity vector; ds is the differential displacement vector over a closed curve and A is the area enclosed.

Chapter 2

2.1 Literature Review

Since the nineteen fifties, many researchers have performed experimental studies to understand the scour process at bridge piers and abutments as well as to derive scour depth predictors. Many studies have been conducted with the goal of predicting scour, and numerous equations have been developed by numerous researchers, including Shen et al. (1969); Breusers et al. (1977); Jain and Fischer (1979); Melville (1992); Liu et al. (1961); Richardson and Richardson (1994); Dey et al. (1995); Muzzammil and Gangadhariah (2003); Marsh *et al.* (2004); Froehlich (1989); Laursen and Toch (1956); Abed and Gasser (1993); Tseng *et al*. (1999); Dey and Raikar (2007); Ashtiani and Kordkandi (2012); Khaple *et al.* (2017) ; Dey (1999); Dey and Raikar (2007); Yilmaz (2017) *et al.*; Graf and Istiarto (2002); Barbhuiya and Dey (2004) etc.

A thorough programme of measurements on the various facets of local scour around piers was carried out by CHABERT and ENGELDINGER (1956). The main factors were velocity, pier shape, grain size (0.26, 0.52, 1.5, and 3.0 m), water depth (0.1 to 0.35 m), and pier diameter (2.5 to 30 cm). Numerous tools to lessen the scour were also tested. Two regimes should be distinguished, according to the study on the influence of flow velocity: for velocities at or below the threshold velocity of movement of the bed material, the scour depth approaches a limit asymptotically. In contrast, the scour depth varies at higher velocities because moving dunes periodically dump material into the scour hole. At speeds close to the threshold velocity, the maximum scour depth was attained , whereas scour initiated at about half the threshold velocity.

Schneider *et al.* (1969) investigated local scour induced by the horseshoe vortex system that occurs at the foot of the piers. The state of the sediment moved into and out of the scour hole serves as the foundation for further categorizing the scour process as clear-water scour or scour with continuous sediment motion. Furthermore, given a continuous uniform flow with fully developed bed material transport, the equilibrium scour depth is dependent on the starting sediment transport condition. Design parameters for blunt-nosed piers under clear-water scour and scour with continuous sediment motion are presented. Several departures from the ideal design circumstances described above are explored, and design techniques for these instances are given.

Dargahi *et al.* (1990) carried out the experimental investigation of clear water scouring around a circular cylinder reveals that the scour mechanism is linked to the three-dimensional separation of the upstream boundary layer and periodic vortex shedding in the cylinder's wake. The first scour develops in the cylinder's wake. A series of horseshoe vortices serves as the primary scouring agent in the upstream area. The vortices have a cyclic nature, resulting in a triple scour profile in the upstream area. The frequency and duration of horseshoe vortex shedding do not alter much during scouring. A robust recurring movement and the production of ripples define the process. The shedding frequency of the wake vortices governs the periodicity. Collars affixed to the cylinder cannot prevent the vortices from forming.

Breusers and Raudkivi (1991) found that reduction of scour depth due to a foundation located at an appropriate level below the initial bed level, should not be reposed on unless: Definite foretelling of bed level are possible, because (the level of the river bed can go down extraordinarily during a flood in a particular spread of the river, or the place of the pier may correspond with that of a moving stream channel in the cross section). This exemplary note, which has been signified by others one of them was Melville (1988) has main implying for design.

Sterling Jones (1992) occurred a study in the laboratory to research the influences of foundation place on the scour depth. The purpose of the study was to find various techniques for describing the pier effectual dimensions or foundation texture when both are displayed to the flow field. The HEC-18 pier-scour equation is a design equation used that contains an implicit over prediction factor 1.2 to 1.3. Both the governing component and weighted pier width techniques are superior to the 10 % depth approach in cases in which the foundation expands into the flow field. This addresses the significant arresting influences of scour caused by foundations placed at or below the bed. Foundations at such places can supply effectual protection against local scour of pier if they are extensive enough.

Fotherby and Jones (1993) classified foundations as deep or shallow, according to whether the foundation was undercut by scour. Deep foundations expand below the base of the scour hole. They displayed that for piers placed on shallow slab foundations the depth of scour was decreased when the foundation was undercut, probably because the stagnation pressures accountable for the formulation of the horseshoe vortex were decreased when the flow could go along down the upstream edge of the foundation. Of course, an undercut foundation is an unfavorable design condition.

Gasser *et al.* (1993**)** conducted a research in which a deep scour hole downstream of a huge circular pier was built at Imbaba bridge, which is regarded one of Cairo's main

Nile River bridges. The Nile River is regarded almost clear at that position, with a fine sand bed. The Hydraulics and Sediment Research Institute (HSRI) in Cairo built an undistorted movable bed model at a scale of 1:60. To explore the reasons of the local scour downstream the circular pier, a series of clear water scour experiments were conducted. The huge scour crater downstream the circular pier was caused by the competing velocity fields at the intersection of the wake vortex streams from nearby piers, and it was exacerbated by the confluence flow. Based on the findings of this study, an empirical formula for predicting the wake and confluence maximum local scour depth downstream of a circular pier in clear water was created.

Melville and Raudkivi (1996) occurred test on nonuniform piers, the non-uniform pier was cylindrical pier place on larger cylinder footing. Besides the factors that influence scour at a uniform pier, the depth of scour at a non-uniform pier is reposed on the ratio D/D*(where D is diameter of pier and D* diameter of foundation) and the depth from the top footing to bed level.

Parola et al. (1996) carried out a search of scouring at piers with rectangular footings. They also noted the preventive ability of foundations place below bed level and indicated on the high sensitivity of depth of scour to footing parameters, especially to the elevation of footing and displayed the influence of rectangular footings over the whole range of possible pier to footing width ratios and through the whole range of footing elevations. They studied the influence of an upstream footing expansion on the scour depth and they attained to conclusion that the expansion of footing in upstream increased the depth of upstream scour decreases.

Dey *et al.* (1999) proposed a theoretical model to estimate the time variation of scour depth in an evolving scour hole at circular piers under clear-water and live-bed scour conditions with uniform and non-uniform sediments based on the concept of the conservation of the mass of sediment, assuming a layer-by-layer scouring process and the horseshoe vortex system as the primary scouring agent. The model closely matches experimental data from various investigators on the time variation of scour depth under clear-water and live-bed scour conditions with uniform and non-uniform sediments.

Melville and Chiew (1999) considered the temporal development of clear-water local scour depth at cylindrical bridge piers in uniform sand beds in their studies. They infer that the scour depth after 10% of the time to equilibrium is between about 50% and 80% of the equilibrium scour depth, depending on the approach flow velocity.

Marsh *et al.* (2004) compared four techniques for forecasting a homogeneous sand bed's incipient motion conditions. (1) the Shields diagram, (2) an empirical technique, (3) a method developed from rotational force resolution, and (4) a simplified rotational force resolution with a variable lift force coefficient are the four ways. For 97 experimental runs from seven different experimental flume investigations, the four approaches were utilized to forecast the incipient motion conditions. Each of the four approaches was assessed in terms of its ability to forecast depth-averaged incipient motion velocity. The Shields approach and the reduced resolution of the rotating forces model were the most successful in forecasting the incipient motion velocity. The slope of the best-fit line for graphs depicting projected vs actual results. Incipient motion velocity was found to be identical (slope = 0.63, 0.65, respectively), demonstrating shows both approaches give a similar level of justification for depth-averaged incipient motion prediction. The empirical approach performed the worst in terms of forecasting observed incipient movement circumstances.

Barbhuiya *et al.* (2005) developed a semi model to compute the fluctuation of scour depth in an emerging scour hole at short abutments (abutment length/flow depth 1), such as the vertical wall, 45° wing wall, and semi - circular, in homogeneous and inhomogeneity sediments under clear water scour conditions, based on the concept of sediment mass conservation, taking into account the scour depth. Experiments were performed out for time variation and 10equilibrium scour depths at various sizes of vertical walls and 45° wing walls.

Raikar *et al.* (2005) investigated clear-water scour at circular and square piers embedded in a sand substrate with a thin armor layer of gravels overlain. Three examples of scour holes at piers in armored beds were identified, based on the pier width, flow depth, armor gravel, and bed-sand sizes. The scour depth at a pier with an armor layer under limited stability of the surface particles is larger than that without an armor layer for the same bed sediments if the secondary armoring is produced inside the scour hole is distributed, according to a comparison of experimental data. For these instances, maximum equilibrium scour depths at piers in armored beds were suggested as equations.

Beg (2010) and Beg and Beg (2015) have studied scour hole characteristics of two piers placed in transverse direction and around two unequal sized bridge piers in tandem arrangement respectively for various spacing of piers. Izadinia *et al.* (2013) studied the structure of turbulence in a scoured bed around a circular pier.

Maity and Mazumder (2014**)** described the turbulent flow statistics over and within the crescentic scour holes induced at the upstream of a horizontal short cylinder placed over the sandy bed transverse to the flow. They analyzed the velocity observations to examine the variation of mean flows, second- and third-order moments, the TKE fluxes, and the turbulent events associated with burst–sweep

cycles and their fractional contributions to the Reynolds stress across the scour holes developed by different cylinder diameters.

The flow pattern and features in a local equilibrium scour around a group of identical circular piers placed eccentrically were the subject of an experimental research by Das *et al.* (2015). At this instance, in the equilibrium condition of a single pier, the eccentricity and longitudinal spacing were equivalent to three times the pier width and 0.5 times the scour affected length, respectively. At the eccentric rear pier, the maximum depth of the scour was almost 44% larger than in the case of a single pier. Additionally, the maximum depth of the scour hole upstream of the inline front pier was almost 29% greater than in the case of a single pier.

Das and Mazumdar (2015) carried out an experimental study to investigate the horse-shoe vortex and flow characteristics in a local equilibrium scour hole around two identical cylindrical piers placed along the flow with an eccentricity and concluded that the eccentric arrangement of piers play an important role in the formation of greater scour depth at the eccentric rear pier.

Das *et al.* (2015) examined the local equilibrium scour features around a set of two identical circular, square, and triangular-shaped piers positioned in the flow's longitudinal direction with a constant eccentricity (transverse distance). The study's major goal was to investigate how the kind of scouring changed as a result of the mutual interference of one pie on another with various longitudinal distances of 0.25, 0.375, 0.5, 0.625, and 0.75 times the scour-affected lengths for a single pier test. The study of the results was primarily concerned with the change of specific non-dimensional equilibrium scour parameters with effective pier width.

Das *et al.* (2016) conducted 19 clear water scour tests to determine the equilibrium scour geometry around two circular, square, and equilateral triangle piers positioned in an in-line front and eccentric rear arrangement. The eccentricity was kept constant while the longitudinal spacing (l) varied between 0.25, 0.375, 0.5, 0.625, and 0.75 times the maximum equilibrium scour-affected length for a single-pier test (L). The maximum scour depth at the eccentric rear pier is determined to be around 45–60% larger than that in the single-pier scenario at l = 0.75L. Furthermore, when l = 0.75L, the maximum depth of the scour hole upstream of the in-line front pier is approximately 35% greater than in the single-pier case.

Yang *et al.* (2016) studied numerically the characteristics of flow patterns around three identical cylinders and the influence of different arrangements of cylinders to suppress the vortex shedding at different Reynolds numbers.

Das *et al.* (2019) investigated a relative scour condition around three-pier group. It is identified the upstream downstream scour geometries when two tandem piers are placed inline and third pier is placed eccentrically in middle of tandem piers. Laboratory scale experiments were physically performed by gradually varying the intermediate longitudinal spacing in between tandem piers. After each experimental run, the scour formation around the pier group and the dune formation downstream of the pier group are investigated.

Chapter 3

3.1 Local Scour Mechanism

The boundary layer flow past a cylindrical pier undergoes a three-dimensional separation. This separated shear layer rolls up along the obstruction to form a vortex system in front of the element which is swept downstream by the river flow. Viewed from the top, this vortex system has the characteristic shape of a horseshoe and thus called a horseshoe vortex Fig 3.1. The formation of the horseshoe vortex and the associated down flow around the cylindrical pier results in increased shear stress and hence a local increase in sediment transport capacity of the flow. This leads to the development of a deep whole (scour hole) around the cylindrical pier, which in turn, changes the flow pattern causing a reduction in shear stress by the flow thus reducing its sediment transport capacity. The temporal variation of scour and the maximum depth of scour at bridge elements therefore mainly depend on the characteristics of flow, pier and river-bed material. The formation of the horseshoe vortex and the associated down flow cause scour at cylindrical pier, abutment and spur dike.

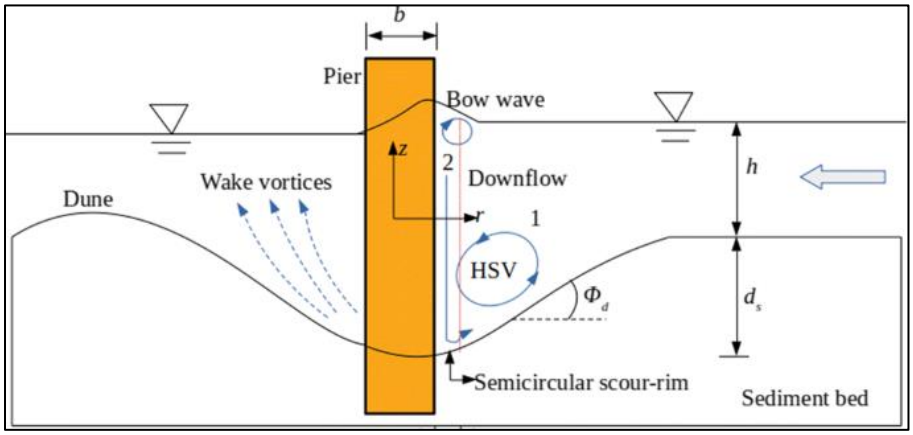

Fig 3.1 Scour mechanism at cylindrical pier

The mechanism of scour around bridge piers were studied by Kothyari *et al.* (1992*a*,*b*) whereas studies on the mechanism of scour around abutments and spur dikes are available in Kothyari and Ranga Raju (2001).

3.2 Horseshoe Vortex And Downflow

The flow deflected by sediment embedded bridge piers causes scour at its foundations. Scour may endanger the stability of the complete bridge structure. In bridge hydraulics circular-shaped pier foundations are commonly used. Due to the similar flow structures of airflow around circular bodies in wind tunnels, the basic researches concern flow visualization in aerodynamics. The main flow features involve a vertically deflected flow along the cylinder front, a horseshoe vortex system upstream of the cylinder, a flow separation beside the cylinder and a wake zone downstream of it shown in Fig. 3.2 For all flow conditions a horseshoe vortex system consisting of at least two vortices.

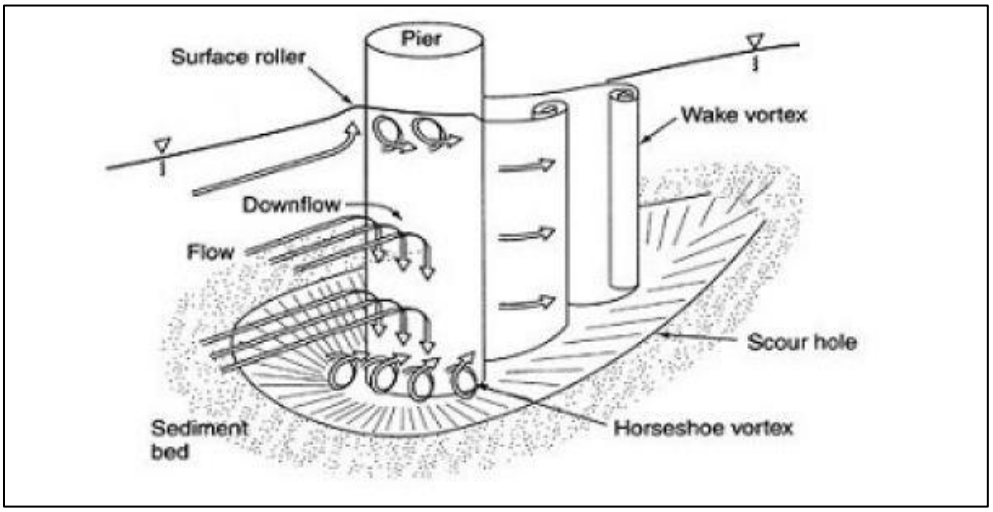

Fig 3.2 Mechanism of horse shoe vortex

Horseshoe vortex in front of the pier to be the prime agent causing scour as said by Kothyari *et al.* (1992) assuming a layer-by-layer scouring process as said by Dey (1999). Tseng *et al.* (1999) said near the upstream face of the pier there exists a downflow which joins the separated flow to form the horseshoe vortex stretched around the pier.

3.3 Wake Vortex

Wake vortices form at the downstream side of piers and are the result of flow separation at the sides of the pier. Called cast-off vortices by Raudkivi (1986), these have vertical axes. One vortex develops on one side, sheds away, and is convected downstream. Immediately, other forms on the other side, finally shedding also. The wake vortices dissipate as they move downstream. The frequency of vortex shedding is directly proportional to the approach velocity and inversely proportional to the pier diameter.

Information on wake vortex scour at bridge piers is particularly scanty. As wake vortex scour occurs at the downstream of the pier, it has little or no destructive potential. Because the horseshoe vortex scour occurs at the face of the pier and threatens to undermine the pier, this type of scour has been given considerable theoretical thought Bruesers *et al.* (1977), and is well-documented with model studies Raudkivi (1986).

Knowledge about wake vortex scour due to bridge piers has come mainly from a few laboratory tests Melville (1975). To describe the scouring action, Melville wrote "each of the concentrated vortices acts with its low pressure center as a vacuum cleaner", picking up material from the bed, which is then transported downstream.

At most bridges, wake vortex scour is insignificant and confluence scour does not exist. In clear-water Rivers flowing on fine sand, these two forms of local scour can be very large. The deep scour holes downstream from the large circular piers (10 and 15 m in diameter) at the Tahrir and Imbaba Bridges over the Nile River in Cairo, Egypt were produced by the conflicting velocity fields at the intersection of the wake vortex streams from adjacent piers. The depths of scour due to these wake vortices are now 8 to 11 m where the normal depth of flow is approximately 8 m. Confluence scour where the main and side channel join upstream from the Imbaba Bridge was 9 m in 1981 and 1987 and was aligned with the bisector of the intersection angle of the two channels. These depths of scour can be considered nearly clear-water scour as the bridges are in the backwater of the Delta Barrages, the velocity is less than 1 m/s and sediment transport is very low. There is concern that the holes may enlarge or move upstream endangering the piers and the bridges. We have made observations in the vicinity of the scour holes and have come to the conclusion that, in each case, the scour was caused by two streams of wake vortices from adjacent piers intersecting downstream. The vortices that result from the two conflicting velocity fields create local scour. At one bridge, the scour is enhanced by the vortices that

occur at the confluence of the main channel and its side channel. This is known as confluence scour.

3.4 Classification Of Scour Parameters

3.4.1 Flow Intensity

Flow intensity is defined as the ratio of the shear velocity (u_*) to the critical shear velocity (u_{*_c}) or the ratio of the approach mean velocity to the critical mean velocity [Melville and Chiew (1999)]. Under clear-water condition, the local scour depth in uniformly-graded sediment increases almost linearly with velocity to a maximum at the threshold velocity [Melville and Coleman (2000)]. The maximum scour depth is reached when the ratio u_*/u_{*_c} = 1 and the corresponding maximum scour depth is called the threshold peak. As the velocity exceeds the threshold velocity, the local scour depth in uniform sediment first decreases and then increases again to a second peak, but the threshold peak is not exceeded provided the sediment is uniform.

3.4.2 Flow Depth

The influence of flow depth on the scour depth has been discussed by many authors [e.g. Breusers and Raudkivi (1991); Melville and Coleman (2000)]. The presence of the pier in the channel causes a surface roller around the pier and a horseshoe vortex at the base of the pier. Flow depth affects local scour depth when the horseshoe vortex is affected by the formation of the surface roller (or bow wave) that forms at the leading edge of the pier. The two rollers, (i.e., the bow wave and the horseshoe vortex) rotate in opposite directions. In principle, as long as there is no interference between the two rollers, the local scour depth does not depend on the flow depth but depends only on the pier diameter.

In such an instance, often called deep flow, the local scour is said to occur at narrow piers. As the flow depth decreases, the surface roller becomes relatively more dominant and causes the horseshoe vortex to be less capable of entraining sediment.

Therefore, for shallower flows, the local scour depth is reduced. Subsequently, in a very shallow flow, the local scour is dependent on the flow depth and the local scour is said to occur at a wide pier.

3.4.3 Pier Width

Experiments have clearly shown that it is possible to relate the scour depth to the size of the pier [Breusers et al. (1977)]. This observation can be explained physically by the fact that scouring is due to the horseshoe vortex system whose dimension is a function of the diameter of the pier. It has also been observed that the horseshoe vortex, being one of the main scouring agents, is proportional to the pier Reynolds number (R_e), which in turn is a function of the pier diameter.

For the same value of mean approach flow velocity, therefore, the scour depth is proportional to the pier width. The influence of pier size on the local scour depth is of interest when data from the laboratory are interpreted for field use [Breusers and Raudkivi (1991)].

Under clear-water conditions, pier size influences the time taken to reach the ultimate scour depth but not its relative magnitude y_s/D, if the influence of relative depth, y_o/D, and relative grain size D/d_{50} on the local scour depth are excluded [Breusers and Raudkivi (1991)]. They also concluded that the volume of the local scour hole formed around the upstream half of the perimeter of the pier is proportional to the cube of the pier diameter (or the projected width of the pier). The larger the pier the larger the scour hole volume and also the longer is the time taken for the development of the scour hole for a given shear stress ratio.

3.4.4 Pier Shape

Piers are constructed of various shapes. The most common shapes used are circular, rectangular, square, rectangular with chamfered end, oblong, Lenticular and Joukowski. The effect of pier shape has been reported by many researchers [e.g. Breusers (1977), Breusers and Raudkivi (1991), Melville and Coleman (2000)].

The blunter the pier, the deeper the local scour has been the general conclusion. The shape of the downstream end of the pier is concluded to be of little significance on the maximum scour depth. The pier shape is often accounted for by using a shape

factor. Melville and Chiew (1999) discussed on shape factors for uniform piers that is piers having constant section throughout their depth, was proposed. The local scour depths for variety of different pier shapes all having the same projected width (140 mm). From his results, a circular pier produced the least scour while a rectangular pier having blunt ends produced the most scour.

For piers tapered on the upstream and downstream faces, the slope, in elevation, of the leading edge of the pier affects the local scour depth. Downward-tapered piers induce deeper scour than does a circular pier of the same width.

3.4.5 Sediment Size

The effects of the grain size and the density of the sediment material are often expressed as a function of the critical flow velocity for the initiation of sediment motion. Breusers and Raudkivi (1991) reported on the work of Raudkivi and Ettema (1977a,b) in which the effect of sediment size on local depth of scour at a bridge pier was studied. The experiments were conducted under clear-water conditions and using a pier of diameter 7 cm and a flume 1.5 m in width. It was observed that a sediment size of $d_{50} \leq 0.7$ mm leads to a formation of ripples, whereas sediment size of $d_{50} \geq 0.7$ mm does not cause ripples. It was further stated that the results for grain sizes which lead to the formation of ripples ($d_{50} \leq 0.7$ mm) were different from those for larger grain sizes for which ripples do not form ($d_{50} \geq 0.7$ mm).

According to Raudkivi and Ettema, for non-ripple- forming sediments ($d_{50} \geq 0.7$ mm), experiments can be run successfully with a flow condition, $u_* \sim 0.95 u_{*c}$, without the upstream bed being disturbed by the approach flow, whereas with finer sands ($d_{50} < 0.7$ mm) a flat bed cannot be maintained for the same flow condition. Therefore, if the sediment is uniform sand with grain size $d_{50} < 0.7$ mm, a flat bed cannot be maintained near the threshold shear stress condition because ripples will develop, with a small amount of general sediment transport taking place so as to replenish some of the sand scoured at the pier. Thus, true clear-water scour conditions cannot be maintained for this case.

3.4.6 Flow Froude Number

The Froude number is a dimensionless number comparing inertia and gravitational forces. It may be used to quantify the resistance of an object moving through water and compare objects of different sizes. Named after William Froude, the Froude number is based on the speed/length ratio as defined by him.

$$F_r = \frac{U}{\sqrt{gh}} \qquad \text{....(3.1)}$$

where U is a characteristic velocity and For rectangular cross-sections with uniform depth h , For F_r < 1 the flow is called a subcritical flow, further for F_r > 1 the flow is characterized as supercritical flow. When $F_r \approx 1$ the flow is denoted as critical flow .

3.4.7 Densimetric Froude Number

The densimetric Froude number is define as $F_r = \frac{U}{\sqrt{g' h}}$

where g' is the reduced gravity $g' = g\frac{\rho_s - \rho_f}{\rho_f}$

where g = acceleration due to gravity

The theoretical critical value is unity, therefore, if F_r >1, no saline wedge will form. In practice, values of F_r as well as 0.6 to 0.7 prevent the formation of a saline wedge. Therefore, for the condition F_r < 0.6, a salt wedge will form.

3.5 Angle Of Repose

The angle of repose, also referred to as angle of friction, is an engineering property of granular materials. The angle of repose is the maximum angle of a stable slope determined by friction, cohesion and the shapes of the particles. When bulk granular materials are poured onto a horizontal surface, a conical pile will form. The internal angle between the surface of the pile and the horizontal surface is known as the angle of repose and is related to the density, surface area, and coefficient of friction of the

material. Material with a low angle of repose forms flatter piles than material with a high angle of repose. In other words, the angle of repose is the angle a pile forms with the ground.

Angle of repose is the steepest angle which the surface of a mass of loose particulate matter makes with the ground. Angle of repose is affected by the size, mass, angularity, and dampness of the particles and by the force of downward acceleration, but it is consistent for a given material. Knowing the angle of repose of a material in various circumstances is vital for engineers and landscapers, for example.

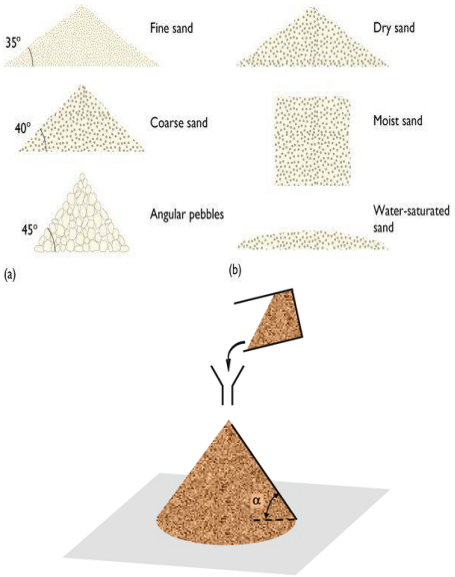

Fig 3.5 Angle of repose

The way in which most people are familiar with angle of repose is sand castles. Dry sand generally has an angle of repose of about 30°, so piled dry sand forms shallow inverted cones. When sand is dampened, the surface tension of the water binds the grains together, and the angle of repose is increased to more than vertical, so that walls and towers and sea caves can be made. When sand is too wet, however, the water lubricates the grains instead of sticking them together, and the angle of repose is decreased to nearly zero. This should be required knowledge for anyone who is thinking of buying a house built on a sandbar.

Chapter 4

4.1 Objective

The main goal of this study is to conduct experiments to demonstrate how the scouring varies around two eccentrically positioned circular piers. In the current study, attempts have been made to observe the nature of the scour depth that is developing around circular piers with respect to time. By adjusting the eccentricity between the piers, six experiments have been run with a fixed pier diameter of 0.07 m and a constant inflow depth of 14.7 cm. The results of the experiments have been carefully analyzed to obtain the pier arrangement in which the maximum scouring is taking place by calculating the scour volume in each case. The experimental procedure followed is as under:

Table 4.1 series of experiments conducted

Pier shape	Experiment /Test no.	Discharge (Q) (Lps)	flow depth (h) (cm)	Pier diameter (b) (cm)	Spacing between piers	
					longitudinal	eccentric
circular	1	27	14.7	7	5.185b	2 b
	2					2.25 b
	3					2.5 b
	4					2.75 b
	5					3 b
	6					3.5 b

4.2 Methodology

1) The flow depth in the flume was adjusted by a tailgate. The approaching flow depth (h) was maintained as 0.147 m for all the tests by operating the tailgate. The bed slope S_0 $(=1:2400)$ was kept constant throughout all the experiments.

2) The critical condition of the bed was examined before test run using steps 2 to 6. The depth-averaged approaching flow velocity (U) was estimated using Manning's equation $\left(U=\frac{1}{n}R^{\frac{2}{3}}S^{\frac{1}{2}}\right)$. Here, the coefficient of roughness (n) was determined by using Strickler's formula $\left(n=\frac{1}{24}d_{50}^{\frac{1}{6}}\right)$. From the sieve analysis test, median diameter of sand (d_{50}) was determined as 0.0784 cm.

3) The critical bed shear stress (τ_{0c}) was determined by using the expression for critical Shields parameter, Θ_c $\left(=\frac{\tau_{0c}}{\Delta\rho_f gd}\right)$ which was developed by Van Rijn (1984). From Van Rijn's (1984) empirical equations of the Shields curve the value of critical Shields parameter was calculated where particle parameter, D_* $\left(=d\left(\frac{\Delta g}{\nu^2}\right)^{\frac{1}{3}}\right)$ = 22.076. Then the equation of critical bed shear stress becomes as $\tau_{0c}=0.0319\Delta\rho_f gd$ (=0.4084 N/m^2).

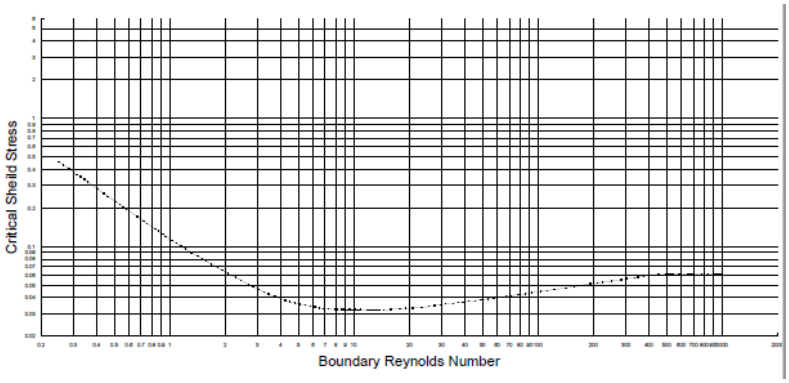

Fig 4.2 shield diagram

5) Then critical shear velocity (u_{*c}) was calculated using $u_{*c} = \sqrt{\frac{\tau_0}{\rho_f}}$. Therefore u_c can be calculated from $\frac{u_c}{u_{*c}} = 5.75\log\left(\frac{h}{2d_{50}}\right) + 6$ where u_{*c}, h, d_{50} are already known.

6) Critical shear flow Reynolds number R_{*c} $\left(= \frac{u_{*c}R}{\nu}\right)$ was determined at 20^0C temperature of water. The below figure shows the Shields' experimental results which relate critical Shields parameter (Θ) and (R_{*c}) and is known as Shields diagram (1936). The threshold of sediment motion occurs when $\Theta > \Theta_c$ or $\tau_0 > \tau_{0c}$ or $u_* > u_{*c}$. From the fig.(4.3) it is clear that the discharge during each test run was lower than the minimum discharge required for the incipient motion or threshold conditions of the bed particles. Therefore, it can be said that all the experiments were carried out under clear water scour condition.

7) The depth-averaged approaching flow velocity (U) was set as about 68% of the critical velocity (u_c) of the uniform sand bed considering side-wall effect to satisfy the clear water condition i.e. the present research considered only clear water approach flow conditions escribed by a threshold/critical Froude number of $F_t = \left(\frac{U}{u_c}\right)$ = 0.68 [Dey and Raikar (2007) and Oliveto and Hager (2002)].The depth averaged approaching flow velocity was determined from the measured vertical profile of the approaching flow velocity at 2 m upstream of the pier where the presence of the pier did not affect the approaching flow. Also to satisfy clear water scour condition, average bed shear stress (τ_0) must be less than or equal to critical bed shear stress (τ_{0c}). It was determined using the method proposed by Dey (2003)

Chapter 5

5.1 Experimental setup

The experimental arrangement, data acquisition system and variables measured in the model study are described. Typical investigation of scour depth development around a bridge pier has been carried out through various experiments. The experimental setup and conditions of the work are described in details. All the experiments are conducted in the Fluvial Hydraulics laboratory of the School Water Resources Engineering department in Jadavpur University, Kolkata.

5.1.1 Tilting Flume

The experiments are carried out in a recirculating flume 11 m long, 0.81 m wide, and 0.60 m deep. The working section of the flume is filled with sand to a uniform thickness of 0.20 m. Length of the sand bed 7m and width 0.81 m. The sand bed is located 2.9 m upstream from the flume inlet. The working section of the flume is made up of a steel bottom and Plexiglas side walls along two sides for most of its length to facilitate visual observations. The recirculating flow system is served by a centrifugal pump located at the upstream end of the flume.

Fig 5.1 Tilting flume used during the experimentation

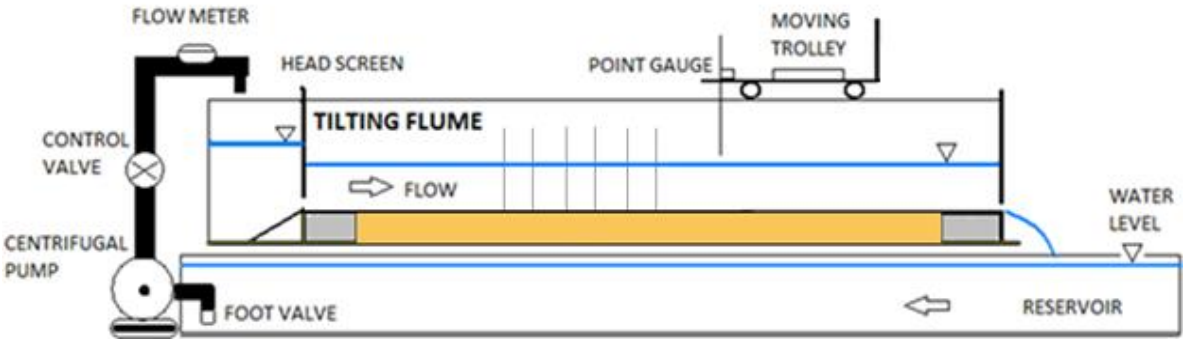

Fig 5.2 Schematic diagram of tilting flume

5.1.2 Pump

The hydraulic machines which convert the mechanical energy in to hydraulic energy are called pumps. The hydraulic energy is in the form of pressure energy. The recirculating flow system is served with a 10hp, variable speed, centrifugal pump located at the upstream end of the flume. Water flows through a 200 mm diameter pipe line which runs directly into the flume. The rpm of the pump is 1430; power 7.5 kW, maximum discharge is 25.5 lps. There are two pumps for alternative used. To measure the discharge, water flows through a flow meter.

Fig 5.3 Pump used to recirculate the flow

5.1.3 Pier

In the present study all three piers was constructed using Perspex sheets. Three circular bridge piers of diameter 7 cm have been used in the present study. The height of the piers is 45.6 cm. During the experiment it is kept in mind that the width of the experimental flume is more than eight times of the pier diameter to avoid the wall friction factor.

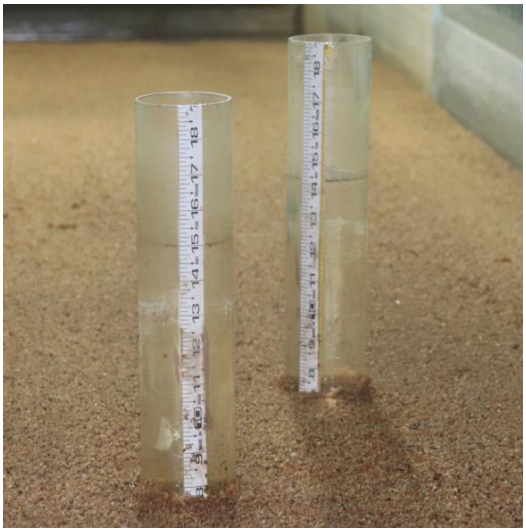

Fig 5.4 Circular Piers of 7 cm diameter

5.1.4 Sand Bed

The shields diagram remains the most effective way of determining threshold conditions for uniform sediments. For given fluid density and viscosity and sediment density, the shields diagram can be used to obtain a plot of shear velocity u_{*_c} against grain size d_{50}. Determination of threshold condition for non-uniform sediment is not so clear cut. The effects of particle size distribution may be important and thus u_c would depend up on both the median grain size d_{50} and the geometric standard deviation, $\sigma_g = \left(d_{84}/d_{16}\right)^{0.5}$ with non-uniform sediments, a flow can disturb the grain, removing some but simply rearranging others into a stable pattern that develops into an armored bed and stabilizes. Such flow is considered here in to be above threshold.

Values of u_c are found using a suggestion first made by Weill that many of the intermediate sizes will move when flow condition based on d_{50} exceed the shields criterion.

Series of tests are carried out on the sand bed material. In the laboratory we measured the vibrating sieve analysis and specific gravity Sand particle size d_{50} is 0.784 mm, d_{16} is 0.5 mm, d_{84} is 1.438 mm and d_{90} is 1.62 mm. Geometric standard deviation of sediment size $\left(\sigma_{\mathrm{g}}\right)$ is 1.8. Density of the sand is 2.582. We have measured the sand particle size from the graph. Here we plot the grain size distribution and percent finer.

Small triangular sand waves with long gradual upstream slope (approximately 6^0) and short steep downstream slope (approximately 32^0) are called ripples. In case of fine sediments (d_{50} < 0.7 mm), ripples are formed, while coarse sediments usually form dunes. The wave lengths of ripples are usually shorter than 300 mm or approximately equaling $150\,d_{50}$. It is assumed that ripples are formed if viscous sub-layer is present when the threshold shear stress is just suppressed, while dunes are formed if the bed is hydraulically rough. The length of the ripples depends on the sediment size and the flow velocity, but is essentially independent of the flow depth. Ripples may be superposed upon the upstream side of dunes.

Dunes are the bed –forms larger than ripples, whose profile is out of phase with the free surface profile. The stream wise profile of a dune is roughly triangular with a mild upstream slope and a downstream slope approximately equal to the angle of repose. Dunes are formed in coarse sediment (d_{50} > 0.6 mm).

Above this a zone of high turbulence exists, where a large production (and dissipation) of turbulent energy takes place. Near the zone of reattachment, the sediment particles are transported by the turbulence, even when the local bed shear stress is below its threshold value. On the upstream side of the dune, the bed shear stress drives sediment particles uphill until they pass over the crest and eventually are buried in the bed for a period. As sediment is transported from the upstream side and deposited on the lee side of a dune, the result is a slow continuous downstream migration of the dunes.

Fig 5.5 Sand bed

After placing the piers in proper position with proper alignment properly flat sand bed was prepared. A very good experiment requires properly prepared flat sand bed which is very essential for attaining good experimental result. A 3 m long and 0.81 m wide flat sand bed was prepared and the flatness of the sand bed was checked with spirit level. The sand bed preparation was done for every new setup of piers arrangement.

5.2 EXPERIMENTAL PROCEDURE

In the present study investigation of scour depth around three identical circular shaped piers have been carried out. The experimental setup and conditions for the study are described in details. All the experiments were conducted in the Fluvial Hydraulics Laboratory of the School of Water Resources Engineering in Jadavpur University.

The experiments were carried out in a recirculating flume. The flume bed was filled with sand to a uniform thickness of 0.20 m, length of the sand bed 3 m and width 0.81 m. The sand bed was located 2.9 m upstream from the flume inlet. The recirculating flow system was served by a centrifugal pump which was located at the upstream end of the tilting flume. The water discharge was measured by a flow meter connected to the upstream pipe at the inlet of the flume. Water flows through a 0.2 m diameter pipe line which runs directly into the flume.

Fig 5.6 Working section of the flume

The average bed shear stress was 0.39 Pa and angle of repose of bed sand and critical bed shear stress were estimated 36^0 and 0.40 Pa respectively. The flow depth in the flume was adjusted by operating a tailgate. The depth averaged approaching flow velocity was found out from the measured vertical profile of the approaching flow velocity at 2 m upstream of the pier where the presence of the pier did not affect the approaching flow.

Froude number $\left(F_{\mathrm{r}}\right)$, flow Reynolds number $\left(R_{\mathrm{e}}\right)$ and pier Reynolds number $\left(R_{\mathrm{p}}\right)$ for all the experiments were calculated as 0.223, 2.4×10^4 and 1.8×10^4 respectively.

The pier is first installed in the flume at the desired location. Before each test, care is taken to level the sand bed throughout the entire length of the flume and perpendicular in the around a pier structure. First of all, we have to produce a sand bed having a smooth, uniform surface, so we used a spirit level to check the uniformity of the bed surface. Uneven bed surface is leveled using a hand trowel. After that we have to measure the bed level by point gauge randomly and to check the leveling of the flume. The sand bed preparation is very key as for as the experiment is concerned. Unevenness or defect in the channel bed can cause the damage the experiment. Piers are constructed in eccentrically with different condition with the help of single pier total scour length.

During the experiment it was kept in mind that the width of the experimental flume is more than seven times of the pier width to avoid the wall friction factor. The minimum value of the ratio between flume width and pier width is 6.25, proposed by

Raudkivi and Ettema (1983) that could be used without a measurable effect from the side walls on the local scour at the pier.

To start the test, the flume is slowly filled with water to the required depth from downstream. It should be noted that extra care is required when filling the flume with water, especially for test of this nature where no sediment movement is allowed. Any deformity in the bed surface may develop of ripples or dunes and general movement of the sand if the shear stress on the smooth bed is close to the critical shear stress. The pump is then turned on and desired flow rate has been achieved by controlling the control valve and a bypass valve.

Concurrent with getting the pump up to speed, the tailgate is adjusted so as to maintain the correct depth (0.125 m) of flow in the flume. Throughout the test period, the location and magnitude of the point of maximum scour depth are around the upstream of the pier. The frequency of the scour depth varied throughout the test period. Rate of scouring is maximum in the period of 1^{st} to 12^{th} hour and then less frequently thereafter. Here we have used the fiber transferring pier model. The run duration for all the experiments is 12 hours. After that the pump is stopped to allow the flume to slowly drain without disturbing the scour topography. The flume bed is then allowed to dry, during which time photo of the scour topography around the pier are taken.

Chapter 6

6.1 Results and discussions

A study of local erosion around two eccentric circular piers in clear-water conditions was carried out. After conducting all the six tests for scour holes geometrical parameters like maximum scour depth, length of sediment shifted to the downstream, max-width of scouring deposition, hole surface area and the total volume of scouring deposited and scour volume was analyzed. Here total experiments were run for a total duration of 12 hours. The scour depth was measured with a help of a laser distance meter and the data obtained was analyzed with the help of surfer software to generate contour maps.

In this present study, the hydrodynamic consequences of different eccentric arrangements on scouring were investigated. Erosion and deposition patterns were studied around the front and eccentric piers at different time intervals along the flume. Total six experiments were carried out with the same experimental conditions such as discharge, velocity, water depth, bed material. The width of each pier was taken 7 cm.

Each experiment was started with a flattened bed. While the outlet valve was closed, the flume was filled with water very slowly without disturbing the bed material, until the desired flow depth was reached. Then the inflow valve was adjusted to the desired discharge in the flume and the outlet valve was partially opened. The experiments were carried out for constant discharge of 27 lit/sec and constant flow depth maintained at 14.7 cm for each discharge. The experimental run duration for each experiment was 12 hours. Knowing that scour depth evolves rapidly at the beginning of the experiments and gets slower towards the end, the scour depth measurements are recorded more frequently at the beginning. In each experiment, the time series were frequent at the beginning such as 2,4,6,8,10,14,18,22,26,30 mins

In order to plot the contour profile, the water in the flume was drained after the completion of experiments and the sediment deposition was investigated by taking the depth at scoured region with the help of laser distance meter. This procedure is repeated for the aforementioned test durations and experiments. The experimental outcomes are discussed below.

Table 6.1: The parameter which are kept constant throughout the series of experiments

Parameter	Values
Flow depth (h)	14.7 cm
Discharge (Q)	27 lps
Longitudinal distance (l_o)	5.19b
Pier width (b)	7cm
Experimental duration (t)	12 hours

6.1.1 Experiment No. 1

Fig 1a: Level bed, Eccentricity e = 2b

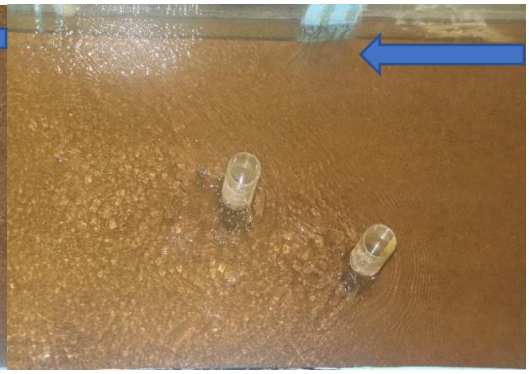

Fig 1b: During Experiment, Eccentricity e = 2b

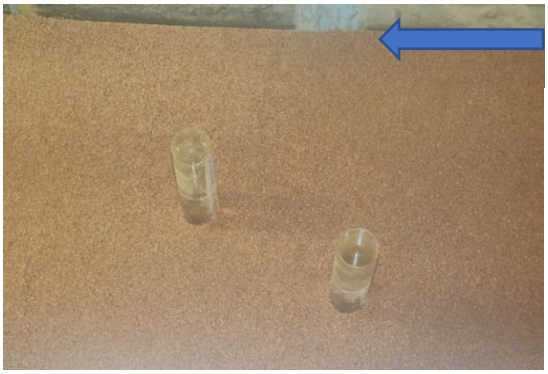

Fig 1c: Scour bed, Eccentricity e = 2b.

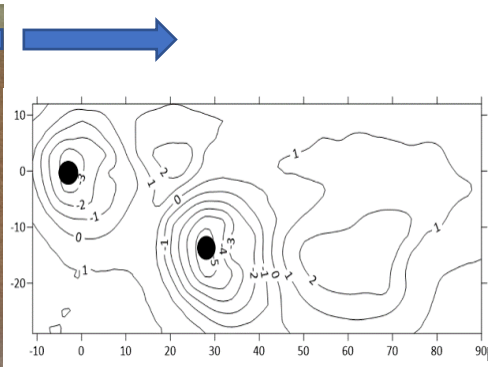

Fig 1d: Contour Map, Eccentricity e = 2b.

This experiment was conducted for an eccentricity of 2b for 12 hours. The values of subsequent scour depths were recorded with a help of laser distance meter. The frequency of recording the scour depths was incremented with the passing of each hour. It was observed that the scour depth for both the piers in this case

was maximum among the series of experiments conducted. The scour depth observed at the front pier was 0.0688 m and that at the eccentric pier was 0.0941m, after the completion of experiment. The contour map was generated using surfer software.

6.1.2 Experiment No. 2

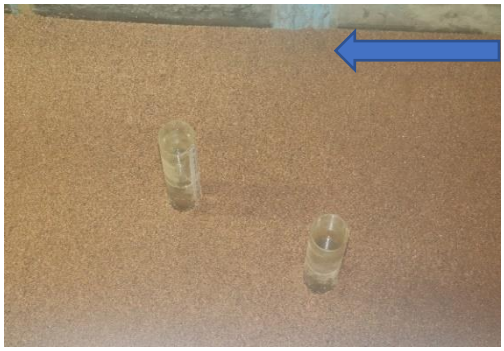

Fig 2a: Level bed, Eccentricity e = 2.25b

Fig 2b: During Experiment, Eccentricity e = 2.25b

Fig 2c: Scour bed, Eccentricity e = 2.25b

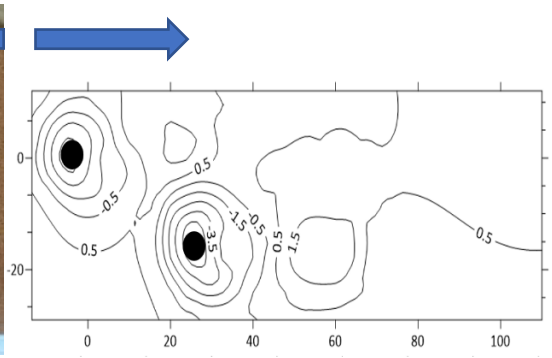

Fig 2d: Contour Map, Eccentricity e = 2.25b

This experiment was conducted for an eccentricity of 2.25b for 12 hours. The values of subsequent scour depths were recorded with a help of laser distance meter. The frequency of recording the scour depths was incremented with the passing of each hour. The scour depth observed at the front pier was 0.0618 m and that at the eccentric pier was 0.0822 m , after the completion of experiment surfer software was used to generate contour maps.

6.1.3 Experiment No. 3

Fig 3a: Level bed, Eccentricity e = 2.5b

Fig 3b: During Experiment, Eccentricity e = 2.5b

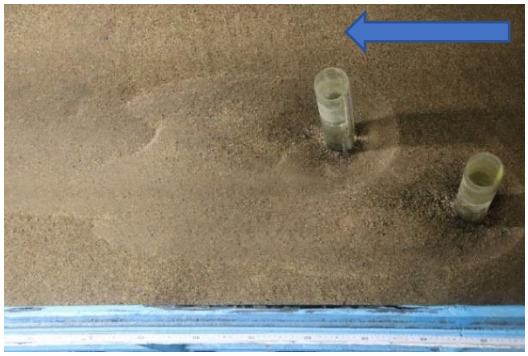

Fig 3c: Scour bed, Eccentricity e = 2.5b.

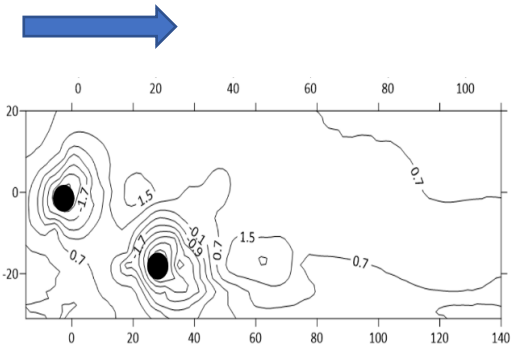

Fig 3d: Contour Map, Eccentricity e = 2.5b

This experiment was conducted for an eccentricity of 2.5b for 12 hours. The values of subsequent scour depths were recorded with a help of laser distance meter. The frequency of recording the scour depths was incremented with the passing of each hour. It was observed that the maximum scour depth in this experiment was very close to the previous experiment i.e., e= 2.25 b. The scour depth observed at the front pier was 0.0655 m and that at the eccentric pier was 0.0822 m, after the completion of experiment.

6.1.4 Experiment No. 4

Fig 4a: Level bed, Eccentricity $e = 2.75b$

Fig 4b: During Experiment, Eccentricity $e = 2.75b$

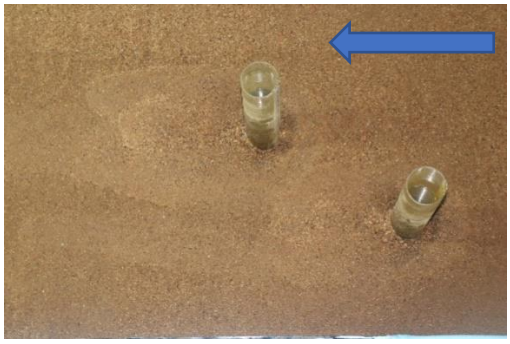

Fig 4c: Scour bed, Eccentricity $e = 2.75b$

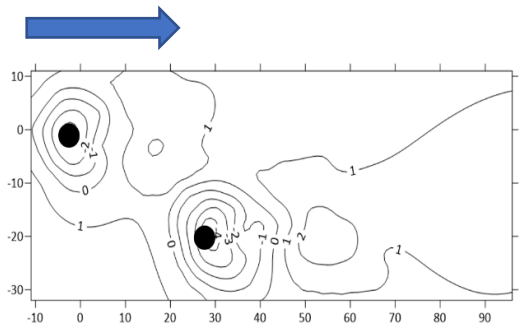

Fig 4d: Contour Map, Eccentricity $e = 2.75b$

This experiment was conducted for an eccentricity of $2.75b$ for 12 hours. The values of subsequent scour depths were recorded with a help of laser distance meter. The frequency of recording the scour depths was incremented with the passing of each hour. It The scour depth observed at the front pier was 0.0662 m and that at the eccentric pier was 0.0839 m, after the completion of experiment.

6.1.5 Experiment No. 5

Fig 5a: Level bed, Eccentricity $e = 3b$

Fig 5b: During Experiment, Eccentricity $e = 3b$

Fig 5c: Scour bed, Eccentricity $e = 3b$.

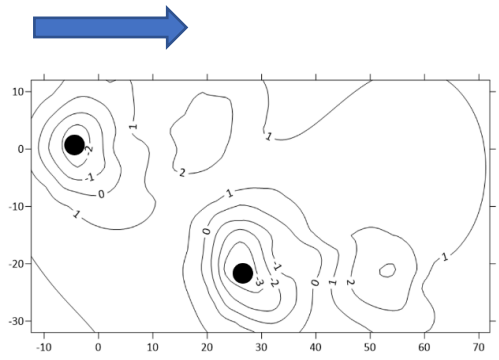

Fig 5d: Contour Map, Eccentricity $e = 3b$.

This experiment was conducted for an eccentricity of $3b$ for 12 hours. The values of subsequent scour depths were recorded with a help of laser distance meter. The frequency of recording the scour depths was incremented with the passing of each hour. The maximum scour depth observed at the front pier was 0.0586 m and that at the eccentric pier was 0.0642 m, after the completion of experiment.

6.1.6 Experiment No. 6

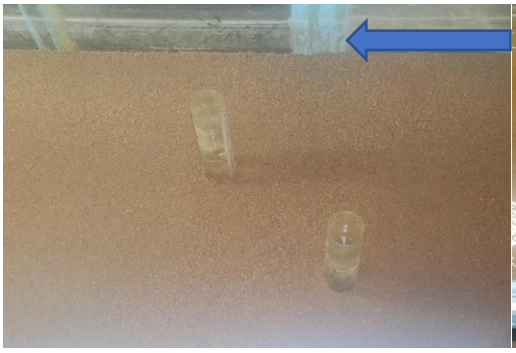

Fig 6a: Level bed, Eccentricity e = 3.5b

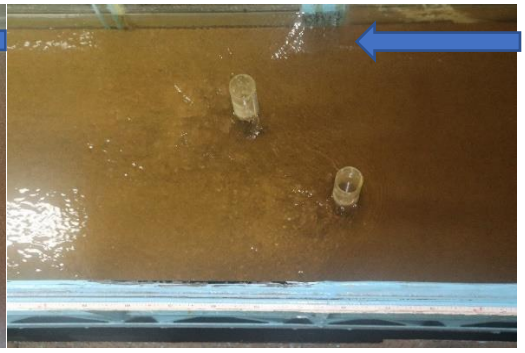

Fig 6b: During Experiment, Eccentricity e = 2b

Fig 6c: Scour bed, Eccentricity e = 3.5b

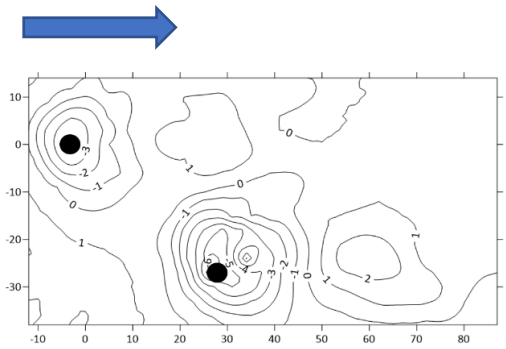

Fig 6d: Contour Map, Eccentricity e = 3.5b

This experiment was conducted for an eccentricity of 3.5b for 12 hours. The values of subsequent scour depths were recorded with a help of laser distance meter. The frequency of recording the scour depths was incremented with the passing of each hour. The maximum scour depth observed at the front pier was 0.0581 m and that at the eccentric pier was 0.0735 m, after the completion of experiment.

Summarizing the values obtained from equilibrium scour parameters for this test are listed below:

Table 6.2: Experimental outcomes

Test No	e (cm)	b (cm)	d_{sf} (cm)	d_{se} (cm)	L_{sf} (cm)	L_{se} (cm)	w_{sf} (cm)	w_{se} (cm)	a_{ps} (cm^2)	a_{ss} (cm^2)	V_s (cm^3)
1	2b	7	6.88	9.41	23.8	28	23.4	28.6	2629.6	2590.7	2172.9
2	2.25b	7	6.18	8.22	26.2	30	32.4	31.8	4019.1	4047	3031.8
3	2.5b	7	6.55	8.22	24.5	79.5	25.6	38.31	4899	4930.9	4258.2
4	2.75b	7	6.62	8.39	17.37	23.88	19.54	24.5	3917	3949.4	4265.9
5	3b	7	5.86	6.42	22.5	22.47	29	23.15	3145.2	3183.4	4089.9
6	3.5b	7	5.81	7.35	23.3	104.69	28.35	39.16	3546.7	3584.2	2690.8

Chapter 7

7.1 CONCLUSIONS

Local scour around eccentric bridge piers in an alluvial channel is a complicated problem, with relatively little success in modelling the local scour computationally. As a result, the physical model remains the most effective method for estimating local scour depth. The physical model data demonstrate that eccentricity and pier geometry have a significant impact on local scour at the bridge pier location. The inline and eccentric spacing of the pier can make a significant difference in reducing the local scour depth.

The maximum scour depth around two circular piers, positioned in eccentric arrangement, is determined by carrying out six clear water scour experiments. Here the inflow depth was kept constant with the varying eccentric spacing from 2, 2.25, 2.5, 2.75,3 and 3.5 times the pier diameter (*b*).

- At eccentricity e =2*b*, the maximum scour depth at the eccentric rear pier is found about 45% greater than that in the case of e =3*b*. The pier arrangement and the interference between the horseshoe vortex of the rear pier and the wake vortex of the front pier may also play an important role in the creation and formation of the greater scour depth at the eccentric rear piers.
- In addition, at e= 2*b*, the maximum depth of the scour hole at the upstream or in-line front pier is about 17% more than that in the case of eccentricity e = 3*b*, which produces minimum scour depth in both the cases.

7.2 FUTURE SCOPE OF THE STUDY

In the current study scour depth data was analyzed by keeping the inflow depth constant. Further analysis can be done by varying the inflow depth along with the eccentricity. More studies can be done based on the variation of longitudinal inline spacing along with eccentricity. Because a bridge pier can be built on soil other than cohesion-less soil, analyzing the performance of a collar as well as the temporal development of scour in cohesive soil will provide useful insight into the behavior of a collar in this situation. Scour can be reduced by using collars. Collars are not only excellent at reducing scour, but they are also far less expensive when compared to countermeasure measures such as riprap. It should also be noted that utilizing a collar induced a delay in the scouring mechanism, and increasing the size of the collar increased the delay time. As the pier spacing grows, the region between the piers without protection is washed away, resulting in greater scour holes at the back piers.

7.3 References

1) A. P. Arabani and H. Hajikandi, (2015). Reduction of Local Scour Around a Bridge Pier using triple Rectangular Plates. *Current World Environment*, Vol. 10, Issue 1, pp.47-55. http://dx.doi.org/10.12944/CWE.10.

2) A.J. Raudkivi and R. Ettema,(1985). Scour at Cylindrical Bridge Piers in Armored Beds. *Journal of Hydraulic Engineering*, Vol. 109, Issue 3, pp.338-350. DOI: 10.1061/(ASCE)0733-9429(1985)111:4(713)

3) A.J. Odgaard and Y. Wang, (1991). Sediment Management with Submerged Vanes. I: Theory. *Journal of Hydraulic Engineering*, Vol. 117, Issue 3, pp. 267-283.

4) A.J. Odgaard and Y.Wang, (1991). Sediment Management with Submerged Vanes I: Applications. *Journal of Hydraulic Engineering*, Vol. 117, Issue 3, pp. 284-302.

5) A.K. Barbhuiya and S. Dey, (2004). Local scour at abutments: a review. *Sadhana*, Vol.29, pp. 449-476.

6) A.Keshavarzi, C. K. Shrestha, M. R.Z Ahedani, J. Ball and H. Khabbaz, (2017, a). Estimation of maximum scour depths at upstream of front and rear piers for two in-line circular columns. *Environ Fluid Mech*, https://doi.org/10.1007/s10652-017-9572-6.

7) A.Keshavarzi, C. K. Shrestha, M. R.Z Ahedani, J. Ball and H. Khabbaz, (2017,b). Experimental study of flow structure around two in-line bridge piers. Ice Institute of Civil Engineers. http://dx.doi.org/10.1680/jwama.16.00104

8) A. M. Yanmaz, H. D. Altinbilek, (1991). Study of time-dependent local scour around bridge piers. *Journal of Hydraulic Engineering*, Vol. 117, Issue 10, pp. 1247–1268.

9) B. A. Ashtiani, Z. B. Ghorghi, and A. A. Beheshti, (2010). Experimental investigation of clear-water local scour of compound piers. *Journal of Hydraulic Engineering*, Vol. 136, Issue 6, pp. 343–351.

10) B. A. Ashtiani and A. A. Kordkandi, (2012). Flow field side-by-side piers with and scour without hole.*European Journal of Mechanics B/Fluilds*, Vol. 36, pp.152-166.

11) B. A. Ashtiani, A. A. Kordkandi, (2013). Flow field around single and tandem piers. Flow.*Turbulence Combust*, Vol. 90, Issue 3, pp. 471–490.

12) B. Ghorbani and J. A. Kells, (2008). Effect of submerged vanes on the scour occurring at a cylindrical pier. *Journal of Hydraulic Research*, Vol. 46, Issue 5, pp. 610-619.

13) B. Liang, S. Du, X. Pan and L. Zhang, (2019). Local Scour for Vertical Piles in Steady Currents: Review of Mechanisms, Influencing Factors and Empirical Equations. *Journal of Marine Science and Engineering.*

14) B. Nandi, S. Das and A. Mazumdar, (2020). Time Variation Analysis of Scour around Eccentrically Placed Three Tandem Cylindrical Piers, Second ASCE India Conference on "Challenges of Resilient and Sustainable Infrastructure Development in Emerging Economies" (CRSIDE2020).

15) B. W. Melville and Y. M. Chiew, (1999).Time scale for local scour at bridge piers. *Journal of Hydraulic Engineering*, Vol. 125, Issue 1, pp. 59-65.

16) B. W. Melville and A. J. Raudkivi, (1977). Flow characteristics in local scour at bridge piers. *Journal of Hydraulic Research*, Vol. 15, Issue 4, pp. 373-380.

17) C. Flokstra, (2006). Modelling of submerged vanes. *Journal of Hydraulic Research*, Vol. 44, Issue 5, pp. 591-602.

18) D.M Sheppard, G. Zhao, and T.H. Copps, (1995). Local scour near multiple pile piers in steady currents. Proceedings of ASCE, International Conference on Water Resources Engineering, San Antonio, USA.

19) G. Lončar, V. Andročec, S. Klapčić and I. Mišura , (2018). Scour around the Circular and Square Profile Piers. Jubilee Annual 2017-2018 of the Croatian Academy of Engineering.

20) H. Fouli and. I. H. Elsebaie, (2016). Reducing local scour at bridge piers using an upstream subsidiary triangular pillar. *Arab Journal of Geoscience*, Vol. 9, pp. 598. DOI 10.1007/s12517-016-2615-3

21) H. Jaman, S. Das, R. Das and A. Mazumdar, (2017). Hydrodynamics of flow obstructed by inline and eccentrically-arranged circular piers on a horizontal bed surface. *Journal of The Institution of Engineers (India):* Series A. DOI: 10.1007/s40030-017-0187-1.

22) H. Jaman, S. Das, A. Kuila and A. Mazumdar, (2017). Hydrodynamic flow patterns around three inline eccentrically arranged circular piers. *Arabian Journal for Science and Engineering*. DOI: 10.1007/s13369-017-2536-9.

23) H.T Ouyang, J.S. Lai, H. Yu and C.H Lu, (2008). Interaction between submerged vanes for sediment management.*Journal of Hydraulic Research*, Vol . 46, Issue 5, pp. 620-627.

24) H. Ouyang , (2009). Investigation on the Dimensions and Shape of a Submerged vane for Sediment Management in Alluvial Channels. *Journal of Hydraulic Engineering*,
Vol. 135, Issue 3, pp. 209-217.

25) H.T. Ouyang and C.P. Lin, (2016). Characteristics of interactions among a row of submerged vanes in various shapes.*Journal of Hydro-environment Research*, Vol. 13, pp. 14-25.

26) H. Wang, H. Tang , Q. Liu Q and Zhao, (2019). Topographic Evolution around Twin Piers in a Tandem Arrangemen KSCE. *Journal of Civil Engineering*. DOI 10.1007/s12205-019-0585-1.

27) M . Burkow and M . Griebel , (2016)**.** A full three dimensional numerical simulation of the sediment transport and the scouring at a rectangular obstacle . *Computers and Fluids* , Vol. 125, pp. 1–10.DOI: 10.1016/j.compfluid.2015.10.014.

28) M. S. Bajestan , K . Khademi and K. Hossein, (2015). Submerged vane-attached to the abutment as scour counter measure .*Ain Shams Engineering Journal* , Vol. 118, Issue 3. DOI: 10.1016/j.asej.2015.02.006.

29) M. Pandey and Z. Ahmad, (2017). .Evaluation of existing equations for temporal scour depth around circular bridge piers . Article in Environmental Fluid Mechanics .
DOI: 10.1007/s10652-017-9529-9.

30) M. Yilmaz, A. M. Yanmaz and M. Koken, (2017). Clear-water scour evolution at dual bridge piers. *Canadian Journal of Civil Engineering*. DOI: 10.1139/cjce-2016-0053.

31) P. A. Johnson, R. D. Hey, M. Tessier and D. L. Rosgen, (2001). Use of Vanes for Control ofScour at Vertical Wall Abutments. *Journal of Hydraulic Engineering*, Vol. 127, Issue 9, pp.772-778.

32) P. Khwairakpam, S. S. Ray, S. Das, R. Das and A. Mazumdar, (2012). Scour Hole Characteristics Around a Vertical Pier Under Clear Water Scour Conditions. *ARPN Journal of Engineering and Applied Sciences*, Vol.7, Issue 6, pp. 649-654.

33) P.L. Narayana, P.V. Timbadiya and P.L. Patel, (2020). Bed level variations around submerged tandem bridge piers in sand beds. *Journal of Hydraulic Engineering*.
DOI: 10.1080/09715010.2020.1723138.

34) R. Das, P. Khwairakpam, S. Das and A. Mazumdar, (2014). Clear-Water Local Scour Around Eccentric Multiple Piers to shift the Line of Sediment Deposition. *Asian Journal of Water, Environment and Pollution*, Vol. 11, Issue 3, pp. 47-54.

.

35) R. Das, S. Das, H. Jaman and A. Mazumdar, (2018). Impact of Upstream Bridge Pier on the Scouring Around Adjacent Downstream Bridge Pier. *Arabian Journal for Science and Engineering.* https://doi.org/10.1007/s13369-018-3418-5

36) S. Das, R. Midya, R. Das and A. Mazumdar, (2013). A Study of Wake Vortex in the Scour Region around a Circular Pier. *International Journal of Fluid Mechanics Research*, Vol. 40, Issue 1, pp. 42-59.

37) S. Das, R. Das and A. Mazumdar, (2014). Variations in clear water scour geometry at pier of different effective widths. *Turkish Journal of Engineering & Environmental Sciences*, Vol. 38, pp. 97- 111.

38) S.Das and A. Mazumdar, (2015). Comparison of Kinematics of Horseshoe Vortex at a Flat two Eccentric Piers of Different Shapes. *Arabian Journal for Science and Engineering*, Vol. 41, Issue 4, pp. 1193-1213.

39) S. Das and A. Mazumdar, (2015). Turbulence flow field around two eccentric circular piers in scour hole. *International Journal of River Basin Management*, Vol. 13, Issue 3, pp. 343–361.

40) S. Das, R. Das, R. Mukherjee and A. Mazumdar, (2017). Enhancement of sediment transportation by increasing scour around a square pier with vane attached on one side: 37th IAHR world congress. Kuala Lumpur.

41) S. M. Ghaneeizad, E.B. Jovein, J. Abrishami and J. F. Atkinso, (2018). Redistribution of flow velocity in sharp bends using unsubmerged vanes. *International Journal of River Basin Management*, DOI: 10.1080/15715124.2017.1411928.

42) W. Y. Chang, G. Constantinescu, H.C.Lien, W.F.Tsai, J.S. Lai and C.H.Loh, (2013).Flow structure around bridge piers of varying geometrical complexity. *Journal of Hydraulic Engineering*, Vol.139, Issue 8, pp. 812-826.

43) Y. Yang, S. M. ASCE, B. W. Melville, M. ASCE, D. M. Sheppard, A. M. ASCE, and A. Y. Shamseldin, (2019). Live-Bed Scour at Wide and Long-Skewed Bridge Piers in Comparatively Shallow Water. *American Society of Civil Engineers.* DOI: 10.1061/(ASCE)HY.1943-7900.0001600.

44) Y. Yang, M. Qi, X. Wang and J. Li, (2019). Experimental study of scour around pile groups in steady flow. https://doi.org/10.1016/j.oceaneng.2019.106651.

45) U.C. Kothyari and A Kumar, (2012). Temporal variation of scour around circular compound piers. *J Hydraulic Eng*, Vol. 138, pp. 945–957, 2012